

This discussion paper is/has been under review for the journal Atmospheric Chemistry and Physics (ACP). Please refer to the corresponding final paper in ACP if available.

Impact of vehicular emissions on the formation of fine particles in the Sao Paulo Metropolitan Area: a numerical study with the WRF-Chem model

A. Vara-Vela¹, M. F. Andrade¹, P. Kumar^{2,3}, R. Y. Ynoue¹, and A. G. Muñoz^{4,5}

¹Department of Atmospheric Sciences, Institute of Astronomy, Geophysics and Atmospheric Sciences, University of São Paulo, São Paulo, Brazil

²Department of Civil and Environmental Engineering, Faculty of Engineering and Physical Sciences (FEPS), University of Surrey, Guilford GU2 7XH, UK

³Environmental Flow (EnFlo) Research Centre, Faculty of Engineering and Physical Sciences, University of Surrey, Guildford GU2 7XH, UK

⁴International Research Institute for Climate and Society (IRI), The Earth Institute, Columbia University, NY, USA

⁵Centro de Modelado Científico (CMC), Universidad del Zulia, Maracaibo, Venezuela

A numerical study
with the WRF-Chem
model

A. Vara-Vela et al.

Title Page

Abstract

Introduction

Conclusions

References

Tables

Figures

◀

▶

◀

▶

Back

Close

Full Screen / Esc

Printer-friendly Version

Interactive Discussion



Received: 23 January 2015 – Accepted: 26 April 2015 – Published: 20 May 2015

Correspondence to: A. Vara-Vela (angel.vela@iag.usp.br)

Published by Copernicus Publications on behalf of the European Geosciences Union.

ACPD

15, 14171–14219, 2015

A numerical study
with the WRF-Chem
model

A. Vara-Vela et al.

Title Page	
Abstract	Introduction
Conclusions	References
Tables	Figures
◀	▶
◀	▶
Back	Close
Full Screen / Esc	
Printer-friendly Version	
Interactive Discussion	



Abstract

The objective of this work is to evaluate the impact of vehicular emissions on the formation of fine particles ($\text{PM}_{2.5}$; $\leq 2.5 \mu\text{m}$ in diameter) in the São Paulo Metropolitan Area (SPMA) in Brazil, where ethanol is used intensively as a fuel in road vehicles. Weather

- 5 Research and Forecasting with Chemistry (WRF-Chem) model is used as photochemical modelling tool to describe the physico-chemical processes leading to evolution of number and mass size distribution of particles through gas-to-particle conversion. A vehicular emission model based on statistical information of vehicular activity is applied to simulate vehicular emissions over the studied area. The study period during a month,
10 between 7 August and 6 September 2012, is considered to perform the numerical simulations due to the availability of experimental data from the NUANCE-SPS (Narrowing the Uncertainties on Aerosol and Climate Changes in São Paulo State) project that aims to characterize emissions of atmospheric aerosols in the SPMA. Results show that the emission of primary gases from vehicles led to a production between 20 and
15 30 % due to new particles formation in relation to the total mass concentration of $\text{PM}_{2.5}$ in the downtown SPMA. Dust and sea-salt aerosols contributed with 40–50 % of the total PM_{10} (PM_{10} ; $\leq 10 \mu\text{m}$ in diameter) concentration. Furthermore, ground level O_3 concentration decreased by about 2 % when the aerosol-radiation feedback is taken into account. Over 40 % of the formation of fine particles, by mass, was due to the emission of hydrocarbons, mainly aromatics. An increase in the number of small particles impaired the ultraviolet radiation and induced a decrease in ozone formation. Availability of experimental measurements of atmospheric aerosols and the application of the WRF-Chem model, which simulates feedbacks between meteorological variables and chemical species, made possible to represent some of the most important properties
20 of fine particles in the SPMA such as the mass size distribution and chemical composition in addition to evaluate its formation potential through the gas-to-particle conversion processes.
25

[Title Page](#)[Abstract](#)[Introduction](#)[Conclusions](#)[References](#)[Tables](#)[Figures](#)[|◀](#)[▶|](#)[◀](#)[▶](#)[Back](#)[Close](#)[Full Screen / Esc](#)[Printer-friendly Version](#)[Interactive Discussion](#)

1 Introduction

A number of past studies has shown the significant participation of the carbonaceous compounds in the concentration of fine particles in the São Paulo Metropolitan Area (SPMA) in Brazil (Albuquerque et al., 2011; Miranda and Andrade, 2005; Ynoue and Andrade, 2004; Castanho and Artaxo, 2001). Studies conducted on ambient air pollution in the SPMA have also shown that black carbon (BC) explains 21 % mass concentrations of fine particles ($\text{PM}_{2.5}$; $\leq 2.5 \mu\text{m}$ in diameter) compared with 40 % of organic carbon (OC), 20 % of sulfates, and 12 % of soil dust (Andrade et al., 2012). A recent report from the São Paulo Environmental Protection Agency (CETESB) highlighted that, in 2012, the vehicles contributed about 40 % of the total $\text{PM}_{10} \leq 10 \mu\text{m}$ in diameter mass concentrations through direct emissions (CETESB, 2013). If we consider the secondary aerosols, which were about 25 % of PM_{10} as per the estimates of CETESB (2013), these were mainly found to form by chemical reactions between gases released from exhaust of vehicles. These observations also allow to conclude that road vehicles represent the main sources of PM_{10} in the SPMA. SPMA has a significant fleet (~ 7 million) of vehicles, which is dominated by light-duty vehicles fueled with gasohol (a mixture of 80 % of gasoline and 20 % of ethanol), pure ethanol, and flex-fuel (any percentage of gasoline and ethanol).

The implementation of the Program for the Control of Vehicular Emission (PROCONVE) established by the Brazilian Government in the 80's, enforcing measures such as use of catalytic converters and ethanol as additive to gasoline in substitution of lead tetraethyl, led to decrease in emissions of CO and VOCs and hence their ambient concentration. For the NO_x , the decrease in emissions is still under way as the main source is the emission from the diesel fleet. According to CETESB (2013), the road vehicles contributed up to about 97, 87 and 80 % of CO, VOCs and NO_x emissions in 2012, respectively. Recent work of Carvalho et al. (2014) reported a substantial increase in number of vehicles from 1 million in 2000 to almost 7 million in 2014, together with

[Title Page](#)[Abstract](#)[Introduction](#)[Conclusions](#)[References](#)[Tables](#)[Figures](#)[◀](#)[▶](#)[◀](#)[▶](#)[Back](#)[Close](#)[Full Screen / Esc](#)[Printer-friendly Version](#)[Interactive Discussion](#)

**A numerical study
with the WRF-Chem
model**

A. Vara-Vela et al.

[Title Page](#)[Abstract](#)[Introduction](#)[Conclusions](#)[References](#)[Tables](#)[Figures](#)[|◀](#)[▶|](#)[◀](#)[▶](#)[Back](#)[Close](#)[Full Screen / Esc](#)[Printer-friendly Version](#)[Interactive Discussion](#)

Title Page	
Abstract	Introduction
Conclusions	References
Tables	Figures
◀	▶
◀	▶
Back	Close
Full Screen / Esc	
Printer-friendly Version	
Interactive Discussion	



An online-coupled meteorology and chemistry model (i.e., the WRF-Chem) has been used to characterize and describe the physico-chemical processes involved in both the formation and growth of new particles over the SPMA in southern Brazil. The details of measurements, WRF-Chem model and emissions are described in Sect. 2. Results from modelling experiments and comparison with measurements are presented in Sect. 3. Finally, the summary and conclusions are given in Sect. 4.

2 Methodology

2.1 Observational datasets

The study period starting from 7 August until 6 September 2012 is selected for comparison with the modelled results (Sect. 2.2) due to the availability of experimental data from the NUANCE-SPS project. The aim of NUANCE-SPS was to evaluate the impact of emissions in the SPMA on the air quality and changing climatic conditions, and feedback mechanisms between climatic perturbations produced by the both primary and secondary emissions and urban atmospheric processes. Aerosol datasets used in this work consists $\text{PM}_{2.5}$ and $\text{PM}_{2.5-10}$, which were collected using a dichotomous sampler and a rotated impactor (MOUDI). The MOUDI impactor collected mass of particles in 10 size classes with nominal 50 % cut-off diameters: 10, 5.6, 3.2, 1.8, 1.0, 0.56, 0.32, 0.18, 0.1 and 0.06 μm . Particles smaller than 0.06 μm were collected in the after filter. The collected filters and substrates were analyzed to the identification of trace elements of mass through X-ray diffraction analysis, mass concentration through gravimetric analysis, and black and organic carbon through reflectance and thermo analysis using a SUNSET OC-EC analyser. Ion concentrations were evaluated through the Ion chromatography analysis of the soluble material collected on the membrane filters (sulphate, nitrate, ammonium, sodium, and chloride). All these samplings were performed on the roof of the main building of the Institute of Astronomy, Geophysics and Atmospheric Sciences of the University of Sao Paulo (IAG-USP), as detailed in Table 1. In

addition, ambient data from the CETESB's air quality monitoring network and the IAG-USP's climatological station (AF-IAG) were also considered for evaluation of numerical simulations. The locations of measurement sites are depicted in Fig. 1 whereas geographic coordinates and the list of pollutants and meteorological parameters monitored at each site is available in Table 2.

2.2 WRF-Chem model

The WRF-Chem model (Grell et al., 2005) is an on-line mesoscale meteorological model, supported by National Center for Atmospheric Research (NCAR) of the USA and several other research institutions around the world. This model is a system of two key components. The WRF-Chem meteorological component, the Weather Research and Forecasting (WRF), is a system configured for both research and operational applications. The dynamical core used in this study is the Advanced Research WRF (ARW). Model's equations into ARW are solved to non-hydrostatic conditions on a fully atmosphere compressible. Further details on the modelling system can be found on the WRF model website (<http://www.wrf-model.org>). On the other hand, the WRF-Chem chemical component treats chemical processes such as dry deposition, gas-phase chemistry, photolysis rates, and aerosols chemistry. A detailed description of the WRF-Chem model can be found on its website (<http://ruc.noaa.gov/wrf/WG11>). Since both meteorological and chemical components are fully coupled, the transport of all chemical species is on-line. The gas-phase chemistry and aerosol modules employed in this study are the Regional Acid Deposition Model, version 2 (RADM2) (Chang et al., 1989) and the Modal Aerosol Dynamics Model for Europe – Secondary Organic Aerosol Model (MADE – SORGAM) (Ackermann et al., 1998; Schell et al., 2001), respectively. The inorganic species included in the RADM2 mechanism are 14 stable species, 4 reactive intermediates, and 3 abundant stable species (oxygen, nitrogen and water). Atmospheric organic chemistry is represented by 26 stable species and 16 peroxy radicals. The RADM2 mechanism represents organic chemistry through a reactivity aggregated molecular approach (Middleton et al., 1990). Similar organic compounds

[Title Page](#)[Abstract](#)[Introduction](#)[Conclusions](#)[References](#)[Tables](#)[Figures](#)[|◀](#)[▶|](#)[◀](#)[▶](#)[Back](#)[Close](#)[Full Screen / Esc](#)[Printer-friendly Version](#)[Interactive Discussion](#)

A numerical study
with the WRF-Chem
model

A. Vara-Vela et al.

[Title Page](#)

[Abstract](#)

[Introduction](#)

[Conclusions](#)

[References](#)

[Tables](#)

[Figures](#)

[◀](#)

[▶](#)

[◀](#)

[▶](#)

[Back](#)

[Close](#)

[Full Screen / Esc](#)

[Printer-friendly Version](#)

[Interactive Discussion](#)



WRF-Chem was configured with three nested grid cells: coarse (75 km), intermediate (15 km) and fine (3 km). The coarse grid covered a big region of Brazil and also of the Atlantic Ocean. The intermediate grid covered the southeast Brazil while the fine grid cell covered barely the SPMA and metropolitan areas nearest to it. Figure 1 shows the arrangement of measurement sites and topography in the downtown area of the 3 km modelling domain. The initial and boundary meteorological conditions are from the National Center for Environmental Prediction's Final Operational Global Analysis with 1° of grid spacing, 26 vertical levels and are available every six hours: 00:00, 06:00, 12:00 and 18:00 UTC (<http://rda.ucar.edu/datasets/ds083.2/>). The initial and boundary chemical global conditions for representing gases and aerosols background concentration are obtained from the Model for Ozone and Related chemical Tracers, version 4 (Emmons et al., 2010). This model was driven by meteorological inputs from the Goddard Earth Observing System Model, version 5 at $1.9^\circ \times 2.5^\circ$ with 56 vertical levels. Table 3 lists the WRF-Chem configuration options employed by this study.

WRF-Chem simulation with coupled primary aerosol (dust and sea-salt) and biogenic emission modules, together with the direct effect of aerosol particles turned on, is performed as the control simulation in order to evaluate the model performance (hereafter referred to as Case_0). For secondary aerosols, a simulation scenario (Case_1) with biogenic and anthropogenic gases emission is performed to evaluate its formation potential. An additional simulation (Case_2) is also performed to evaluate the impact of aerosols on ozone photochemistry. Notation and description of simulations are listed in Table 4.

Title Page	
Abstract	Introduction
Conclusions	References
Tables	Figures
◀	▶
◀	▶
Back	Close
Full Screen / Esc	
Printer-friendly Version	
Interactive Discussion	



2.3 Emissions

2.3.1 Anthropogenic emissions

Anthropogenic emissions of trace gases and particles in both 3 and 15 km grid cells were considered from road vehicles only through the use of a vehicular emission model developed by the IAG-USP's Laboratory of Atmospheric Processes (LAPAt). Basically, this model considers the number of vehicles, vehicular emission factors, and average driving kilometers for vehicle per day as basic parameters for the calculation of exhaust emissions according to CETESB (2012). The details of this model are available in Andrade et al. (2015). In the case of VOCs, there are other two relevant emissions (fuel transfer and evaporative processes) associated with the vehicles, besides the exhaust emissions. Because of the complexities in the spatial representation due to a numerous factors such as emissions at service stations, such emission sources are assumed to be emitted by exhaust of vehicles for the sake of simplicity. The vehicular fleet and intensity of use datasets are provided by the National Department of Traffic (DENATRAN) and the São Paulo Transporte (SPTrans), respectively. Emission factors for road vehicles for most pollutants were considered from previous studies performed inside the road tunnels (i.e. Janio Quadros (JQ) tunnel and the tunnel 3 of the Rodoanel Mario Covas that is referred hereafter as RA tunnel) located within the SPMA (Pérez-Martínez et al., 2014; Nogueira et al., 2014). However, emission factors for VOCs are considered from dynamometer protocols (CETESB, 2010). VOCs and particulate matter speciation profiles used by pas-phase and aerosol chemical modules were also obtained from NUANCE-SPS experimental campaigns performed in 2011 (tunnel measurements) and 2012 (ambient data). It is important to note that due to the lack of information on vehicular emission factors and intensity of use for most of the other metropolitan areas inside both grid cells, the calculation of vehicular emissions for these urban areas was carried out on the basis of the parameters found for the SPMA. The number of vehicles in any grid cell is calculated from the sum of the number of vehicles at each one of the main urban areas inside the grid cell in question.

ACPD

15, 14171–14219, 2015

A numerical study
with the WRF-Chem
model

A. Vara-Vela et al.

[Title Page](#)

[Abstract](#)

[Introduction](#)

[Conclusions](#)

[References](#)

[Tables](#)

[Figures](#)

◀

▶

◀

▶

[Back](#)

[Close](#)

[Full Screen / Esc](#)

[Printer-friendly Version](#)

[Interactive Discussion](#)



**A numerical study
with the WRF-Chem
model**

A. Vara-Vela et al.

[Title Page](#)[Abstract](#)[Introduction](#)[Conclusions](#)[References](#)[Tables](#)[Figures](#)[◀](#)[▶](#)[◀](#)[▶](#)[Back](#)[Close](#)[Full Screen / Esc](#)[Printer-friendly Version](#)[Interactive Discussion](#)

way to assimilate emissions to WRF-Chem. The method is explained in the OLE2 Wiki pages in detail (http://www.cmc.org.ve/mediawiki/index.php?title=Calidad_de_Aire).

2.3.2 Other emissions

Biogenic emissions are calculated online based on the Guenther scheme (Guenther et al., 1993, 1994). The Guenther biogenic emissions model calculates the emission rates using temperature, photo-synthetically active radiation flux and land-use data as the US Geological Survey (USGS) land-use cover system classification if coupled with the WRF model. However, as indicated in the WRF-Chem emissions guide (http://ruc.noaa.gov/wrf/WG11/Emission_guide.pdf), several key chemical species would have been representing relatively low emission rates because of the limited vegetation types in the simulation, and thus their impacts are anticipated to be much lower than those from vehicular emissions.

Dust and sea-salt emissions are calculated online following the works of Ginoux et al. (2001) and Gong (2003), respectively. The calculation of Ginoux et al. (2001) for the uplifting of dust particles is based on the surface wind speed, wetness and information of soil characteristics. The model then solves the continuity equation including the emission, chemistry, advection, convection, diffusion, dry deposition, and wet deposition of each species. The parameterization of sea-salt aerosol source function of Gong (2003) is an extended parameterization of Monahan et al. (1986) which scales the generation of marine aerosols from mechanical disruption of wave crests by the wind and sea surface covered by whitecaps.

3 Results and discussion

3.1 Characterization of meteorological conditions

In order to study and understand the spatial and temporal variability of atmospheric aerosols, O_3 , and other pollutants during the study period, firstly it is necessary to

Title Page

Abstract

Introduction

Conclusions

References

Tables

Figures

◀

▶

◀

▶

Back

Close

Full Screen / Esc

Printer-friendly Version

Interactive Discussion



analyse the behavior of main meteorological systems acting on the atmospheric environment of the SPMA and surrounding areas.

According to the monthly climate reports from the IAG-USP's Climate Research Group (GrEC), the observed precipitation rates were lesser than the climatological value in the São Paulo State during August 2012. Negative anomalies on the precipitation were caused by the intensification of the South Atlantic Subtropical High (SASH). These conditions established an easterly wind anomalies pattern at the 850 hPa level. Conditions were unfavourable for relative humidity comes from the Amazon due to the Low Level Jet (LLJ) and less intense Alisian winds in the Tropical Atlantic. However, the action of frontal systems favoured the rain accumulation in September 2012, mainly in western State where the greater positive amount of anomalies was observed. Precipitation areas were predominantly observed at the second half of the month. In this case, the wind pattern showed an opposite configuration to that observed in August 2012 as a result of the weakening of the SASH. The IAG-USP's climatological station recorded an accumulated precipitation of about 1.3 mm on three days of occurrence (28 August, 30 August and 4 September 2012) and an easterly wind pattern with a median intensity of 2 m s^{-1} during the period between 7 August and 6 September 2012. Figure 3 shows the accumulated daily precipitation and humidity observed at the IAG-USP's climatological station.

3.2 Analysis of aerosol species

Aerosol analysis included species such as organic carbon (OC), elemental carbon (EC), sulphate, nitrate, ammonium, sodium and chloride in addition to other elemental constituent of PM. All the sampling for these species were performed at IAG-USP. Results showed that the major contributors to the concentration of fine particles are OM (55.7 %; OM : OC ratio of 1.5 found by Brito et al., 2013) and EC (15 %), followed by sulphate (2.9 %), ammonium (2.1 %), sodium (1.9 %), nitrate (0.5 %) and chloride (0.3 %). The remaining mass (21.6 %) is calculated by determining of the difference between the total mass of PM_{2.5} (from the gravimetric analysis) and the sum of the masses of

[Title Page](#)[Abstract](#)[Introduction](#)[Conclusions](#)[References](#)[Tables](#)[Figures](#)[◀](#)[▶](#)[◀](#)[▶](#)[Back](#)[Close](#)[Full Screen / Esc](#)[Printer-friendly Version](#)[Interactive Discussion](#)

Title Page	
Abstract	Introduction
Conclusions	References
Tables	Figures
◀	▶
◀	▶
Back	Close
Full Screen / Esc	
Printer-friendly Version	
Interactive Discussion	



7 individual compounds, as noted above. Part of this unexplainable concentration is related to the water content of aerosols.

On the other hand, PM_{2.5}, PM₁₀ and size distribution of particles measured at IAG-USP show that the study period was characterized by a reduction in the concentrations up to the end of August 2012 when their minimum values were achieved. This reduction was related to the action of a semi-stationary front between the coasts of São Paulo and Paraná States. After the passage of this system, aerosol concentrations have significantly increased what could be related to an increase in relative humidity once the SASH system is moved away from the continent. Aerosols coming from forest fires did not significantly contribute to increased PM concentrations during this period.

Figure 4 shows the concentration of OC, EC and some species of PM_{2.5} during the study period at IAG-USP. We can observe eleven exceedances of PM_{2.5} concentration with respect to the air quality standard of 25 µg m⁻³ (see grey line in Fig. 4a) established by the World Health Organization (WHO). These exceedances have mainly occurred at the beginning and at the end of the study period when an increase in the concentrations of OC and BC were observed. Several studies have shown the contribution of forest fires on the atmospheric aerosol concentrations in São Paulo (Vieira-Filho et al., 2013; Vasconcellos et al., 2010). The satellite images taken in 2012 over the São Paulo State by the AQUA_{M-T} detected about 435 fires in August 2012. One way to qualitatively evaluate the contribution of forest fires on aerosol concentrations is by using the air mass trajectories. Figure 5 shows the back trajectory of an air mass and number of forest fires refers to the day on 9 August 2012, when significant increases in the OC and EC concentrations were observed at the measurement site. In both cases, the air mass did not pass through areas of high density fires before reaching to the measurement site. The predicted average surface wind was predominantly from southeast (see Fig. 6). The increasing organic matter could be associated to high vehicular emission events in case of less favourable meteorological conditions (e.g. lower height of lower planetary boundary layer, PBL, or slow transport of air pollutants) that may have led to a more efficient formation of secondary particles.

Size distributions of aerosol mass indicate that majority of sulphate, ammonium and PM₁₀ mass concentration is distributed in the size range with diameters between 0.1 and 1 µm, commonly known as accumulation mode particles (Kumar et al., 2010). In the cases of nitrate, sodium, and chloride, most part of mass was concentrated in particles with diameters greater than 1 µm.

3.3 Comparison of baseline simulation with observations

All the numerical results presented in this section, for the purpose of comparison with the measurements, were obtained from the baseline simulation (Case_0). The predicted temperature, humidity, and wind distribution have been compared to measurements from the AF-IAG and INT measurement sites. Overall, the model captured the diurnal variation of temperature, humidity, and wind directions reasonably well. However, the predicted wind speeds were slightly lower than the observed values. To explore the model performance in solving the meteorology, we computed some performance statistics for predictions of temperature, humidity and wind speeds at the ground level surface. Table 5 presents the summary of these statistics, showing comparisons between WRF-Chem predictions and observations. Figure 6 shows the predicted average temporal variations of wind vectors at 10 m and temperature at 2 m. Blue dots represent the locations of AF-IAG and INT sites, while the numbers in cyan indicate the observed average temperatures (i.e. 17.7 °C at AF-IAG and 17.8 °C at INT). On an average, the predicted wind direction was easterly in SPMA, which has somewhat affected the spatial distribution of aerosol particles as is examined later in this section. Likewise, a good agreement is found between the predicted PM_{2.5}, PM₁₀ and O₃ concentration and measurements at most of the sites. Figures 7–9 show the observed and predicted temporal variations of PM_{2.5}, PM₁₀ and O₃ concentrations at 3, 10 and 6 sites in the SPMA, respectively, with some measurement sites sharing the same grid point for comparisons due to the geographical proximity. These figures suggest that predicted concentrations did not present any significant spatial variation in the downtown SPMA and were generally underestimated when compared to measurements. This un-

A numerical study with the WRF-Chem model

A. Vara-Vela et al.

Title Page

Abstract

Introduction

Conclusions

References

Table

Figures



Back

Close

Full Screen / Esc

[Printer-friendly Version](#)

Interactive Discussion



der prediction could be associated with an underestimation on the vehicular emissions as well as other emission sources (e.g. emissions coming from point sources) that are disregarded in this study. The high concentrations of $\text{PM}_{2.5}$, PM_{10} and O_3 observed at the beginning and at the end of the study period, which were reasonably well captured by the model, would be related with the emission of high aerosol loadings as well as the establishment of lower PBL heights. The results for this simulation (Case_0) show that overall the predicted PBL heights (not shown here) have a regular diurnal variation in the downtown SPMA with values of up to 700 m in the middle of the study period. Statistics to quantify the model performance in the representation of $\text{PM}_{2.5}$, PM_{10} and O_3 concentrations can be visualized along with the Taylor Diagram shown in Fig. 10. The mean biases for $\text{PM}_{2.5}$, PM_{10} and O_3 concentrations were -8.84 , $-14.13 \mu\text{g m}^{-3}$ and -0.85 ppbv , respectively (see Table 5).

Figures 11–13 show the predicted average surface distribution of $\text{PM}_{2.5}$, PM_{10} and $\text{PM}_{2.5} : \text{PM}_{10}$ ratio for the 3 km modelling domain, respectively. Red dots and cyan numbers represent the locations and the observed mean PM concentrations (or mean PM concentration ratios) at the measurement sites, respectively. Major contributions of $\text{PM}_{2.5}$ on the total PM_{10} concentration were observed mainly over offshore continental areas (see Fig. 13). High $\text{PM}_{2.5} : \text{PM}_{10}$ concentration ratios would be firstly associated with the transportation of fine particles and gases from upwind regions (see Fig. 6), followed by a production of fine particles from biogenic emissions. Additional comparisons between the observed and predicted concentrations of OC and EC at IAG-USP (the only site with measurements of OC and EC) are shown in Fig. 14. In addition to an underestimation of emissions, under predicted OC concentrations could also be associated with an underestimation of SOA probably due to the absence of oxidation of monoterpenes and a limited treatment of anthropogenic VOCs oxidation in the RADM2 mechanism, as discussed by Tuccella et al. (2012). The SORGAM aerosol module considers the formation of anthropogenic SOAs from the oxidation of alkane, alkene and aromatic VOCs as well as the biogenic SOA formation from the oxidation of alpha-pinene, limonene and isoprene VOCs. Recent studies coupling non-traditional

Title Page	
Abstract	Introduction
Conclusions	References
Tables	Figures
◀	▶
◀	▶
Back	Close
Full Screen / Esc	
Printer-friendly Version	
Interactive Discussion	



SOA models (volatility basis set approaches) in WRF-Chem show improvements in the predicted SOA concentrations, although these are still lower than those observed (e.g. Li et al., 2011b; Ahmadov et al., 2012; Srivastava et al., 2013).

On the other hand, measurements of mass size distribution were also made by a MOUDI impactor at IAG-USP. Constituents of aerosol were subsequently determined by X-Ray fluorescence analysis. As previously indicated in this section, among the main identified species are SO_4 , NO_3 , NH_4 , Na and Cl. The observed average aerosol composition is derived using measurements from both MOUDI impactor and SUNSET analyzer. To perform the comparisons of mass size distribution, we adequately joined the MOUDI bin sizes according to the three modes used by the MADE aerosol module: Aitken ($< 0.1 \mu\text{m}$), accumulation ($0.1\text{--}1 \mu\text{m}$) and coarse ($> 1 \mu\text{m}$). The observed and predicted aerosol mass size distributions averaged over the same sampling time period (16 days along the study period) are shown in Fig. 15. Over the downtown SPMA, both the observed and predicted fine particles from accumulation mode account for majority of the total $\text{PM}_{2.5}$ mass. Since the formation-growth processes of aerosols in question are explicitly treated in the Aitken and accumulation modes, the predicted concentrations for particles larger than $1 \mu\text{m}$ are assumed to be zero. In this case, the mass of particles larger than $1 \mu\text{m}$ is allocated to the PM_{10} aerosol variable (see Fig. 15). The comparison between the observed and predicted average contributions for the main identified aerosol constituents at the IAG-USP site is shown in Fig. 16. Both the observed and predicted OC and EC make up the largest fraction of $\text{PM}_{2.5}$ mass with contributions around 55 and 40 %, respectively. In addition, it was found that the predicted SOA concentrations contribute 17 % of the predicted total OC concentration at this measurement site. Various global and regional scale SOA simulations have been conducted using mass-based yield and partitioning coefficients, but they have underestimated the SOA concentrations by roughly an order of magnitude, especially over urban regions (Matsui et al., 2014). Using the same SOA formation approach employed by this study and a conversion factor of 1.6 to convert the emissions of OC to OM, Tuccella et al. (2012) found that the simulated SOA:OM ratios were under-

[Title Page](#)[Abstract](#)[Introduction](#)[Conclusions](#)[References](#)[Tables](#)[Figures](#)[|◀](#)[▶|](#)[◀](#)[▶](#)[Back](#)[Close](#)[Full Screen / Esc](#)[Printer-friendly Version](#)[Interactive Discussion](#)

estimated in the range of 5–40 % against 50–80 % observed. Although the predicted average PM_{2.5} concentration (14.48 µg m⁻³) was lower than observed (22.32 µg m⁻³), the mean aerosol chemical composition was reasonably well represented by the model (see Fig. 16).

5 3.4 Impact of dust and sea-salt emissions on PM concentration

The evaluation of the contribution of dust and sea-salt aerosols on PM₁₀ concentration is performed from the sum of their concentrations divided by the PM₁₀ concentration. The simulated average ratio between the sum of dust and sea-salt aerosols concentration and PM₁₀ concentration is shown in Fig. 17b. High concentration ratios have 10 been observed over the ocean where sea-salt emissions are by far the most important aerosols source. Unlike high concentration ratios over the ocean, lower concentration ratios are observed over the continent far away from the coast. In this region, the main sources of atmospheric aerosols would be associated with the emission of primary biological aerosol, SOA formed from the emission of biogenic volatile organic compounds (BVOCs), and forest fires. However, particles could also be transported from remote 15 areas. In addition, we can also observe that dust and sea-salt aerosols have a contribution between 40 and 50 % of the total PM₁₀ concentration in the downtown SPMA. Although not shown here, it is possible to estimate the contribution of all the other PM₁₀ (i.e., the coarse anthropogenic aerosol) to the total PM₁₀ mass concentration. It may 20 be directly calculated from the model. Another way to estimate this contribution is from the Figs. 13 and 17b once the sum of concentrations of PM_{2.5}, dust and sea-salt, and coarse anthropogenic aerosol represents 100 % of the total PM₁₀ mass concentration. For example, we found that the coarse anthropogenic aerosol represents around 10 % of PM₁₀ in the downtown SPMA.

Title Page	
Abstract	Introduction
Conclusions	References
Tables	Figures
◀	▶
◀	▶
Back	Close
Full Screen / Esc	
Printer-friendly Version	
Interactive Discussion	



3.5 Evaluation of secondary aerosol formation

As described in Sect. 2.1, the aerosol module employed by this study (the MADE/SORGAM) includes the homogeneous nucleation in the sulphuric acid-water system. The sulphuric acid is the most significant condensable molecule formed in the atmosphere, which has also been long recognised as the most important molecule from the point of view of the nucleation of new particles (Jenkin and Clemitshaw, 2000; Seinfeld and Pandis, 2006). But for the SPMA, the importance of SOA formed from the anthropogenic emission of fuel used by the transport sector was noted. The subsequent growth processes involve aerosol growth by condensation of condensable material onto existing particles, and by coagulation of particles to form larger particles (Kumar et al., 2011, 2014). For example, particles in the accumulation mode emerge through coagulation of particles from the Aitken mode (Kumar et al., 2011). It is important to emphasize that the boundaries were updated with gas and aerosol background concentrations coming from the 15 km modelling domain during the whole simulation period. Thereafter, the impact of vehicular emissions on the formation of fine particles was performed from the predicted PM_{2.5} concentration considering an emission scenario (Case_1) in which only emission of gases from vehicles and vegetation are taken into account to be emitted to the atmosphere from the surface. The predicted average PM_{2.5} (Case_1) : PM_{2.5} (Case_0) ratio is shown in Fig. 17a. A contribution between 20 and 30 % in the predicted baseline PM_{2.5} concentration in downtown SPMA is found to correspond to the fine particles formation and transportation processes. Higher concentration ratios over the SPMA surroundings (30–50 %) could be associated with more efficient biogenic emissions. Overall, it is observed that the formation efficiency increases toward the northwest from the ocean. Deep red areas in Fig. 17a could also be associated with the transportation of fine particles and gases from other regions, in addition to having a more efficient production of fine particles from biogenic emissions. For example, given the distribution of winds in Fig. 6, the northern boundary could represent the main source of particles and gases over this part of the

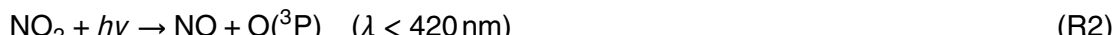
[Title Page](#)[Abstract](#)[Introduction](#)[Conclusions](#)[References](#)[Tables](#)[Figures](#)[|◀](#)[▶|](#)[◀](#)[▶](#)[Back](#)[Close](#)[Full Screen / Esc](#)[Printer-friendly Version](#)[Interactive Discussion](#)

Title Page	
Abstract	Introduction
Conclusions	References
Tables	Figures
◀	▶
◀	▶
Back	Close
Full Screen / Esc	
Printer-friendly Version	
Interactive Discussion	

simulation domain. Additionally, the comparison between the predicted OC and EC concentrations and measurements at IAG-USP is shown in Fig. 14. Considering the Case_1 simulation, we can observe very low concentrations for EC (mean concentration of $0.01 \mu\text{g m}^{-3}$), as expected. This is because these particles are not produced by photochemical processes in the atmosphere, but associated mainly with the diesel exhaust.

3.6 Aerosol impact on O₃ photochemistry

Ozone photochemistry production mainly depends on the two key photolysis rates, as shown in Reactions (R1) and (R2) below (i.e., shortwave radiation able to reach the surface to break molecules of O₃ and NO₂). Therefore, the impact of aerosols on O₃ photochemistry has been evaluated from the impact of aerosols on downward shortwave radiation. Attenuation (scattering and absorption) of downward shortwave radiation by aerosols may substantially modify the photolysis rates, and thereby impacting on the ozone photochemistry production.



The average percentage change in surface O₃ concentrations at 16:00 LT with and without the aerosol-radiation feedback module turned on are shown by Case_0 and Case_2, respectively (Fig. 17c). Overall O₃ is destroyed or formed (incoming transported from other regions) in small quantities between –1 and 1 % in relation to its total concentration. In addition, it was observed that the surface O₃ concentration decreased by around 2 % in the downtown SPMA. Li et al. (2011a) found that the impact of aerosols on O₃ formation in Mexico City was most pronounced in the morning with the O₃ reduction of 5–20 %, but the reduction is less than 5 % in the afternoon. Low reductions in the O₃ concentration in the downtown SPMA compared to results from other studies may be explained by the lower predicted PM₁₀ concentrations, which can lead to a minor attenuation of the incoming solar radiation. Simulated mean downward



[Title Page](#)[Abstract](#)[Introduction](#)[Conclusions](#)[References](#)[Tables](#)[Figures](#)[|◀](#)[▶|](#)[◀](#)[▶](#)[Back](#)[Close](#)[Full Screen / Esc](#)[Printer-friendly Version](#)[Interactive Discussion](#)

short wave fluxes at ground surface (not shown) were up to 5 % higher for the Case_2 than for the Case_0 during the afternoon. The inclusion of the direct effect of aerosol particles was found to have small reductions in the surface temperature (changes by around 2 %), presumably due to an increase in the number of atmospheric processes involving downward long-wave fluxes over this area. Forkel et al. (2012) found an underestimation of predicted downward long-wave radiation over the southern Baltic Sea when the direct effect of aerosol particles was neglected. Despite the highly non-linear behaviour of tropospheric O₃, the reduction in the predicted O₃ concentrations indicates a high efficiency of aerosols to attenuate the downward shortwave radiation what is plausible once it was found that low PM₁₀ concentrations have a capability to reduce ground level O₃ concentrations to a few ppbv. The impact of the fine particles has been discussed in previous works, with evaluation of the scattering and absorbing effects of the aerosol (e.g. Li et al., 2005; Real et al., 2011). Vehicular emissions of particulate matter in the SPMA have a high percentage of Black Carbon (Brito et al., 2013), which after emitted to the atmosphere can enhance the absorption coefficient and thus the attenuation rates.

4 Summary and conclusions

The WRF-Chem community model has been used to evaluate the impact of vehicular emissions on the fine particles formation in the SPMA. Three thirty-one day simulations covering a period from 7 August to 6 September 2012 have been performed. The aims were to evaluate the impact of fine particles formation (both inorganic and SOA) from gases emitted by road vehicles as well as the aerosol impacts on the ozone formation photochemistry. The results are compared with the measurements available from the NUANCE project.

The predicted temporal variations of meteorology, PM_{2.5}, PM₁₀ and O₃ were found to agree well with the measurements at most of the sites during the entire simulation period. However, the predicted concentrations of PM_{2.5} PM₁₀ and O₃ were lower than the

observed values. This difference could be associated with an underestimation of the vehicular emissions and other emission sources such as industry, heating and cooking, which are not considered in this study. Wind speed and direction played an important role in the distribution of fine particles over the simulation domain. The baseline simulation (Case_0) showed that dust and sea-salt aerosols made a contribution between 40 and 50 % of the total PM₁₀ concentration in the downtown SPMA. On the other hand, the Case_1, which represents simulations with gaseous emissions only, indicates that the emissions of primary gases come mainly from vehicles has a potential to form new particles between 20 and 30 % in relation to the baseline PM_{2.5} concentration found in the downtown SPMA. Finally, the Case_2, which represents simulations with aerosol-radiation feedback turned on, reveals a reduction in the surface O₃ concentration by around 2 % when the aerosol-radiation feedback is taken into account.

This study provides a first step to understand the impact of vehicular emissions on the secondary particles formation in the SPMA. Nevertheless, more experimental campaigns are recommended for future work in order to characterize aerosols for their improve emission estimates so that a better understanding of physical and chemical properties and their formation can be established. This study also evaluates the importance of the VOCs in the formation of not only O₃ but also of fine particles. These compounds play an important role concerning health impacts and climate change, and the control of their concentrations requires the description of their formation mechanisms.

Acknowledgements. P. Kumar, A. Vara-Vela and M. de Fatima Andrade thank the University of Surrey's International Relations Office for the Santander Postgraduate Mobility Award that helped A. Vara-Vela to visit University of Surrey, UK, and develop this research article collaboratively. The authors from Universities of Surrey and Sao Paulo also acknowledge the collaborative funding received through the University Global Partnership Network (UGPN) to the project titled "*Emissions And Role Of Fine Aerosol Particles In Formation Of Clouds and Precipitation (eRAIN) – A demonstration study for the megacity, São Paulo*" for supporting this research work. M. de Fatima Andrade and A. Vara-Vela acknowledged funding from the Coordination for the Improvement of Higher Education Personnel (CAPES) and Research Foundation

Title Page	
Abstract	Introduction
Conclusions	References
Tables	Figures
◀	▶
◀	▶
Back	Close
Full Screen / Esc	
Printer-friendly Version	
Interactive Discussion	



of the State of São Paulo (FAPESP, project 2008/58104–8) that allowed the experimental campaigns. The authors also thank the WRF-Chem developers, the NOAA's National Geophysical Data Center, the NCAR's Data Support Section and Atmospheric Chemistry Division, the Latin American Observatory (OLE2), the São Paulo Environmental Protection Agency (CETESB),
5 the OpenStreetMap Data Extracts, and the NCAR Command Language (NCL) software for providing the tools and datasets used in this research.

References

- Ackermann, I. J., Hass, H., Memmesheimer, M., Ebel, A., Binkowski, F. S., and Shankar, U.:
10 Modal aerosol dynamics model for Europe: development and first applications, *Atmos. Environ.*, 32, 2981–2999, 1998.
- Ahmadov, R., McKeen, S. A., Robinson, A. L., Bahreini, R., Middlebrook, A. M., de Gouw, J. A., Meagher, J., Hsie, E. Y., Edgerton, E., Shaw, S., and Trainer, M.: A volatility basis set model for summertime secondary organic aerosols over the eastern United States in 2006, *J. Geophys. Res.*, 117, D06301, doi:10.1029/2011JD016831, 2012.
- 15 Albuquerque, T. T. A., Andrade, M. F., and Ynoue, R. Y.: Characterization of atmospheric aerosols in the city of São Paulo, Brazil: comparisons between polluted and unpolluted periods, *Water Air Soil Poll.*, 195, 201–213, 2011.
- Andrade, M. F., Fornaro, A., Miranda, R. M., Kerr, A., Oyama, B., Andre, P. A., and Saldiva, P.:
20 Vehicle emissions and PM_{2.5} mass concentrations in six Brazilian cities, *Air Qual. Atmos. Health*, 5, 79–88, 2012.
- Andrade, M. F., Ynoue, R. Y., Freitas, E. D., Todesco, E., Vara-Vela, A., Ibarra, S., Martins, L. D., Martins, J. A., Carvalho, V. S. B.: Air quality forecasting system for Southeastern Brazil, *Front. Environ. Sci.*, 3, 1–14, 2015.
- Binkowski, F. S. and Shankar, U.: The regional particulate matter model, 1. mode description
25 and preliminary results, *J. Geophys. Res.*, 100, 26191–26209, 1995.
- Brito, J., Rizzo, L. V., Herckes, P., Vasconcellos, P. C., Caumo, S. E. S., Fornaro, A., Ynoue, R. Y., Artaxo, P., and Andrade, M. F.: Physical–chemical characterisation of the particulate matter inside two road tunnels in the São Paulo Metropolitan Area, *Atmos. Chem. Phys.*, 13, 12199–12213, doi:10.5194/acp-13-12199-2013, 2013.

[Title Page](#)

[Abstract](#)

[Introduction](#)

[Conclusions](#)

[References](#)

[Tables](#)

[Figures](#)

◀

▶

[Back](#)

[Close](#)

[Full Screen / Esc](#)

[Printer-friendly Version](#)

[Interactive Discussion](#)



- Brown, S. G., Lee, T., Roberts, P. T., and Collett Jr., J. L.: Variations in the OM/OC ratio of urban organic aerosol next to a major roadway, *J. Air Waste Manage.*, 63, 1422–1433, 2013.
- Carvalho, V. S. B., Freitas, E. D., Martins, L. D., Martins, J. A., Mazzoli, C. R., and Andrade, M. F.: Air quality status and trends over the Metropolitan Area of São Paulo, Brazil as a result of emission control policies, *Environ. Sci. Policy*, 47, 68–79, 2015.
- Castanho, A. D. A. and Artaxo, P.: São Paulo aerosol source apportionment for wintertime and summertime, *Atmos. Environ.*, 35, 4889–4902, 2001.
- CETESB: Companhia de Tecnologia de Saneamento Ambiental, Relatório Anual de Qualidade do Ar no Estado de São Paulo 2009, São Paulo, 2010.
- CETESB: Companhia de Tecnologia de Saneamento Ambiental, Emissões veiculares no Estado de São Paulo 2011, São Paulo, 2012.
- CETESB: Companhia de Tecnologia de Saneamento Ambiental, Relatório Anual de Qualidade do Ar no Estado de São Paulo 2012, São Paulo, 2013.
- Chang, J. S., Binkowski, F. S., Seaman, N. L., McHenry, J. N., Samson, P. J., Stockwell, W. R., Walcek, C. J., Madronich, S., Middleton, P. B., Pleim, J. E., and Lansford, H. H.: The regional acid deposition model and engineering model, State-of-Science/Technology, Report 4, National Acid Precipitation Assessment Program, Washington, DC, 1989.
- Emmons, L. K., Walters, S., Hess, P. G., Lamarque, J.-F., Pfister, G. G., Fillmore, D., Granier, C., Guenther, A., Kinnison, D., Laepple, T., Orlando, J., Tie, X., Tyndall, G., Wiedinmyer, C., Baugcum, S. L., and Kloster, S.: Description and evaluation of the Model for Ozone and Related chemical Tracers, version 4 (MOZART-4), *Geosci. Model Dev.*, 3, 43–67, doi:10.5194/gmd-3-43-2010, 2010.
- Fast, J. D., Gustafson, W. I., Easter, R. C., Zaveri, R. A., Barnard, J. C., Chapman, E. G., Grell, G. A., and Peckham, S. E.: Evolution of ozone, particulates, and aerosol direct radiative forcing in the vicinity of Houston using a fully coupled meteorology-chemistry-aerosol module, *J. Geophys. Res.*, 111, D21305, doi:10.1029/2005JD006721, 2006.
- Forkel, R., Werhahn, J., Hansen, A. B., McKeen, S., Peckham, S., Grell, G., and Suppan, P.: Effect of aerosol-radiation feedback on regional air quality – a case study with WRF/Chem, *Atmos. Environ.*, 53, 202–211, 2012.
- Ginoux, P., Chin, M., Tegen, I., Prospero, J. M., Holben, B., Dubovik, O., and Lin, S.-J.: Sources and distributions of dust aerosols simulated with the GOCART model, *J. Geophys. Res.*, 106, 255–273, 2001.

[Title Page](#)[Abstract](#)[Introduction](#)[Conclusions](#)[References](#)[Tables](#)[Figures](#)[|◀](#)[▶|](#)[◀](#)[▶](#)[Back](#)[Close](#)[Full Screen / Esc](#)[Printer-friendly Version](#)[Interactive Discussion](#)

- Gong, S. L.: A parameterization of sea-salt aerosol source function for sub- and super-micron particles, *Global Biogeochem. Cy.*, 17, 1097, doi:10.1029/2003GB002079, 2003.
- Gorin, C. A., Collett Jr., J. L., and Herckes, P.: Wood smoke contribution to winter aerosol in Fresno, CA, *J. Air Waste Manage.*, 56, 1584–1590, 2006.
- 5 Grell, G. A., Peckham, S. E., Schmitz, R., McKeen, S. A., Wilczak, J., and Eder, B.: Fully coupled “online” chemistry within the WRF model, *Atmos. Environ.*, 39, 6957–6975, 2005.
- Guenther, A. B., Zimmerman, P. R., Harley, P. C., Monson, R. K., and Fall, R.: Isoprene and monoterpane emission rate variability: model evaluations and sensitivity analyses, *J. Geophys. Res.*, 98D, 12609–12617, 1993.
- 10 Guenther, A., Zimmerman, P., and Wildermuth, M.: Natural volatile organic compound emission rateestimates for US woodland landscapes, *Atmos. Environ.*, 28, 1197–1210, 1994.
- Heal, M. R., Kumar, P., and Harrison, R. M.: Particles, air quality, policy and health, *Chem. Soc. Rev.*, 41, 6606–6630, 2012.
- Jenkin, M. E. and Clemitsaw, K. C.: Ozone and other secondary photochemical pollutants: 15 chemical processes governing their formation in the planetary boundary layer, *Atmos. Environ.*, 34, 2499–2527, 2000.
- Kroll, J. H. and Seinfeld, J. H.: Chemistry of secondary organic aerosol: formation and evolution of low-volatility organics in the atmosphere, *Atmos. Environ.*, 42, 3593–3624, 2008.
- Kulmala, M., Laaksonen, A., and Pirjola, L.: Parameterization for sulphuric acid/water nucleation rates, *J. Geophys. Res.*, 103, 8301–8307, 1998.
- 20 Kumar, P., Robins, A., Vardoulakis, S., and Britter, R.: A review of the characteristics of nanoparticles in the urban atmosphere and the prospects for developing regulatory control, *Atmos. Environ.*, 44, 5035–5052, 2010.
- Kumar, P., Ketzel, M., Vardoulakis, S., Pirjola, L., Britter, R.: Dynamics and dispersion modelling 25 of nanoparticles from road traffic in the urban atmospheric environment – a review, *J. Aerosol Sci.*, 42, 580–603, 2011.
- Kumar, P., Morawska, L., Birmili, W., Paasonen, P., Hu, M., Kulmala, M., Harrison, R. M., Norford, L., and Britter, R.: Ultrafine particles in cities, *Environ. Int.*, 66, 1–10, 2014.
- Li, G., Zhang, R., and Fan, J.: Impacts of black carbon aerosol on photolysis and ozone, *J. Geophys. Res.*, 110, D23206, doi:10.1029/2005JD005898, 2005.
- 30 Li, G., Bei, N., Tie, X., and Molina, L. T.: Aerosol effects on the photochemistry in Mexico City during MCMA-2006/MILAGRO campaign, *Atmos. Chem. Phys.*, 11, 5169–5182, doi:10.5194/acp-11-5169-2011, 2011a.

**A numerical study
with the WRF-Chem
model**

A. Vara-Vela et al.

[Title Page](#)[Abstract](#)[Introduction](#)[Conclusions](#)[References](#)[Tables](#)[Figures](#)[◀](#)[▶](#)[◀](#)[▶](#)[Back](#)[Close](#)[Full Screen / Esc](#)[Printer-friendly Version](#)[Interactive Discussion](#)

- Li, G., Zavala, M., Lei, W., Tsimpidi, A. P., Karydis, V. A., Pandis, S. N., Canagaratna, M. R., and Molina, L. T.: Simulations of organic aerosol concentrations in Mexico City using the WRF-CHEM model during the MCMA-2006/MILAGRO campaign, *Atmos. Chem. Phys.*, 11, 3789–3809, doi:10.5194/acp-11-3789-2011, 2011b.
- McMurtry, P., Shepherd, M., and Vickery, J.: *Particulate Matter Science for Policy Makers: A NARSTO Assessment*, Cambridge University Press, Cambridge, England, 2004.
- Middleton, P., Stockwell, W. R., and Carter, W. P. L.: Aggregation and analysis of volatile organic compound emissions for regional modelling, *Atmos. Environ.*, 24A, 1107–1133, 1990.
- Miranda, R. M. and Andrade, M. F.: Physicochemical characteristics of atmospheric aerosols during winter in the São Paulo metropolitan area in Brazil, *Atmos. Environ.*, 39, 6188–6193, 2005.
- Monahan, E. C., Spiel, D. E., and Davidson, K. L.: A model of marine aerosol generation via whitecaps and wave disruption, in: *Oceanic Whitecaps*, edited by: Monahan, E. C. and Mac Niocaill, G. D., Reidel Publishing Company, Norwell, Mass, 167–174, 1986.
- Muñoz, A. G., López, P., Velásquez, R., Monterrey, L., León, G., Ruiz, F., Recalde, C., Cadena, J., Mejía, R., Paredes, M., Bazo, J., Reyes, C., Carrasco, G., Castellón, Y., Villarroel, C., Quintana, J., and Urdaneta, A.: An environmental watch system for the Andean Countries: el observatorio Andino, *B. Am. Meteorol. Soc.*, 91, 1645–1652, 2010.
- Muñoz, A. G., Ruiz-Carrascal, D., Ramírez, P., León, G., Quintana, J., Bonilla, A., Torres, W., Pastén, M., and Sánchez, O.: Risk management at the Latin American observatory, in: *Risk Management – Current Issues and Challenges*, Intech, 533–556, doi:10.5772/50788, 2012.
- Nogueira, T., Dominutti, P. A., De Carvalho, L. R. F., Fornaro, A., and Andrade, M. F.: Formaldehyde and acetaldehyde measurements in urban atmosphere impacted by the use of ethanol biofuel: Metropolitan Area of São Paulo, 2012–2013, *Fuel*, 134, 505–513, 2014.
- Odum, J. R., Hoffmann, T., Bowman, F., Collins, D., Flagan, R. C., and Seinfeld, J. H.: Gas/particle partitioning and secondary organic aerosol yields, *Environ. Sci. Technol.*, 30, 2580–2585, 1996.
- Pankow, J. F.: An absorption model of the gas aerosol partitioning involved in the formation of secondary organic aerosol, *Atmos. Environ.*, 28, 185–188, 1994a.
- Pankow, J. F.: An absorption model of the gas aerosol partitioning involved in the formation of secondary organic aerosol, *Atmos. Environ.*, 28, 189–93, 1994b.

A numerical study with the WRF-Chem model

A. Vara-Vela et al.

[Title Page](#)

[Abstract](#)

[Introduction](#)

[Conclusions](#)

[References](#)

[Tables](#)

[Figures](#)

◀

▶

[Back](#)

[Close](#)

[Full Screen / Esc](#)

[Printer-friendly Version](#)

[Interactive Discussion](#)



- Pérez-Martínez, P. J., Miranda, R. M., Nogueira, T., Guardani, M. L., Fornaro, A., Ynoue, R., and Andrade, M. F.: Emission factors of air pollutants measured inside road tunnels in São Paulo: case study comparison, *Int. J. Environ. Sci. Te.*, 11, 2155–2168, 2014.
- Real, E. and Sartelet, K.: Modeling of photolysis rates over Europe: impact on chemical gaseous species and aerosols, *Atmos. Chem. Phys.*, 11, 1711–1727, doi:10.5194/acp-11-1711-2011, 2011.
- Saxena, P., Hudishevskyj, A. B., Seigneur, C., and Seinfeld, J. H.: A comparative study of equilibrium approaches to the chemical characterization of secondary aerosols, *Atmos. Environ.*, 20, 1471–1483, 1986.
- Schell, B., Ackerman, I. J., Hass, H., Binkowski, F. S., and Ebel, A.: Modelling the formation of secondary organic aerosol within a comprehensive air quality model system, *J. Geophys. Res.*, 106, 28275–28293, 2001.
- Seinfeld, J. H. and Pandis, S. N.: *Atmospheric Chemistry and Physics: from Air Pollution to Climate Change*, 2nd edn., John Wiley, New Jersey, 2006.
- Shrivastava, M., Berg, L. K., Fast, J. F., Easter, R. C., Laskin, A., Chapman, E. G., Gustafson Jr., W. I., Liu, Y., and Berkowitz, C. M.: Modelling aerosols and their interactions with shallow cumuli during the 2007 CHAPS field study, *J. Geophys. Res.-Atmos.*, 118, 1343–1360, 2013.
- Tuccella, P., Curci, G., Visconti, G., Bessagnet, B., Menut, L., and Park, R. J.: Modelling of gas and aerosol with WRF-Chem over Europe: evaluation and sensitivity study, *J. Geophys. Res.*, 117, D03303, doi:10.1029/2011JD016302, 2012.
- Vasconcellos, P. C., Souza, D. Z., Sanchez-Ccocyollo, O. R., Bustillos, J. O. V., Lee, H., Santos, F. C., Nascimento, K. H., Araujo, M. P., Saarnio, K., Teinila, K., and Hillamo, R.: Determination of anthropogenic and biogenic compounds on atmospheric aerosol collected in urban, biomass burning and forest areas in São Paulo, Brazil, *Sci. Total Environ.*, 408, 5836–5844, 2010.
- Vieira-Filho, M. S., Pedrotti, J. J., and Fornaro, A.: Contribution of long and mid-range transport on the sodium and potassium concentrations in rainwater samples, São Paulo megacity, Brazil, *Atmos. Environ.*, 79, 299–307, 2013.
- Ynoue, R. Y. and Andrade, M. F.: Size-resolved mass balance of aerosol particles over the São Paulo Metropolitan Area of Brazil, *Aerosol Sci. Tech.*, 1, 52–62, 2004.

A numerical study with the WRF-Chem model

A. Vara-Vela et al.

[Title Page](#)

[Abstract](#)

[Introduction](#)

[Conclusions](#)

[References](#)

[Tables](#)

[Figures](#)

◀

▶

◀

▶

[Back](#)

[Close](#)

[Full Screen / Esc](#)

[Printer-friendly Version](#)

[Interactive Discussion](#)



Table 1. Description of aerosol sampling campaigns performed at IAG-USP.

Parameter	Sampling frequency	Period of sampling	Sampling device
Aerosol mass size distribution	24 h	Jul–Sep	MOUDI rotate impactor
PM _{2.5} and PM ₁₀ concentration	12 h	Jul–Sep	PARTISOL sampler
OC and EC concentration	12 h	Aug–Sep	SUNSET analysis



Table 2. Description of measurement sites.

Initials	Name	Latitude	Longitude	Measured species
NSO	Nossa S. do O	-23.4796	-46.6916	PM ₁₀ , O ₃
SAN	Santana	-23.5055	-46.6285	PM ₁₀
PDP	Parque D. Pedro	-23.5448	-46.6276	PM ₁₀ , O ₃
MOO	Mooca	-23.5497	-46.5984	PM ₁₀ , O ₃
CCE	Cerqueira Cesar	-23.5531	-46.6723	PM ₁₀
IAG-USP	IAG-USP	-23.5590	-46.7330	PM ₁₀ , PM _{2.5} , OC, EC Aerosol mass size distrib. ^a
IPEN-USP	IPEN-USP	-23.5662	-46.7374	PM _{2.5} , O ₃ , NO _x , CO
IBI	Ibirapuera	-23.5914	-46.6602	PM ₁₀ , O ₃ , NO _x , CO
CON	Congonhas	-23.6159	-46.6630	PM ₁₀ , PM _{2.5}
AF-IAG	AF-IAG	-23.6500	-46.6167	T, RH, WS, WD ^b
SAM	Santo Amaro	-23.6545	-46.7095	PM ₁₀
INT	Interlagos	-23.6805	-46.6750	PM ₁₀ , O ₃ , T, RH, WS, WD

^a Includes SO₄²⁻, NO₃⁻, NH₄⁺, Na⁺, Cl⁻ and PM₁₀.^b T, RH, WS, and WD denote temperature, relative humidity, wind speed and wind direction, respectively.

Title Page	Abstract	Introduction
Conclusions	References	
Tables	Figures	
◀	▶	
◀	▶	
Back	Close	
Full Screen / Esc		
Printer-friendly Version		
Interactive Discussion		



Table 3. Selected WRF-Chem configuration options.

Atmospheric Process	WRF-Chem option
Longwave radiation	RRTM
Shortwave radiation	Goddard
Surface layer	Monin–Obukhov
Land surface	Noah
Boundary layer	YSU
Cumulus clouds ^a	Grell 3-D
Cloud microphysics	Lin
Gas-phase chemistry	RADM2
Aerosol chemistry	MADE/SORGAM
Photolysis	Fast-J

^a Outer domains only.

- [Title Page](#)
- [Abstract](#) [Introduction](#)
- [Conclusions](#) [References](#)
- [Tables](#) [Figures](#)
- [◀](#) [▶](#)
- [◀](#) [▶](#)
- [Back](#) [Close](#)
- [Full Screen / Esc](#)
- [Printer-friendly Version](#)
- [Interactive Discussion](#)



Table 4. Description of WRF-Chem simulations.

Label	Description
Case_0 (Baseline simulation)	Emission of gases
	Emission of aerosols
Case_1	Aerosol – radiation feedback turned on
	Emission of gases
Case_2	No emission of aerosols
	Aerosol – radiation feedback turned on
	Emission of gases
	Emission of aerosols
	Aerosol – radiation feedback turned off

- [Title Page](#)
- [Abstract](#) [Introduction](#)
- [Conclusions](#) [References](#)
- [Tables](#) [Figures](#)
- [◀](#) [▶](#)
- [◀](#) [▶](#)
- [Back](#) [Close](#)
- [Full Screen / Esc](#)
- [Printer-friendly Version](#)
- [Interactive Discussion](#)



Table 5. Performance statistics for WRF-Chem predictions at all sites.^a

Index	PM _{2.5}	PM ₁₀	O ₃	NO _x	CO	T	RH	U ^b	V ^c
Correlation	0.73	0.72	0.63	0.42	0.54	0.71	0.62	0.48	0.44
Bias	-8.84	-14.1	-0.85	-8.75	-0.27	0.65	-5.74	-0.96	0.75
RMSE _{UB}	6.83	10.59	27.45	30.35	0.57	3.21	20.06	1.04	1.02

^aValues are averaged from all the individual indexes found at the measurement sites. Individual indexes are calculated from both hourly observed and predicted values.

^bZonal wind component.

^cMeridional wind component.

Title Page

Abstract

Introduction

Conclusions

References

Tables

Figures

|◀

▶|

◀

▶

Back

Close

Full Screen / Esc

Printer-friendly Version

Interactive Discussion



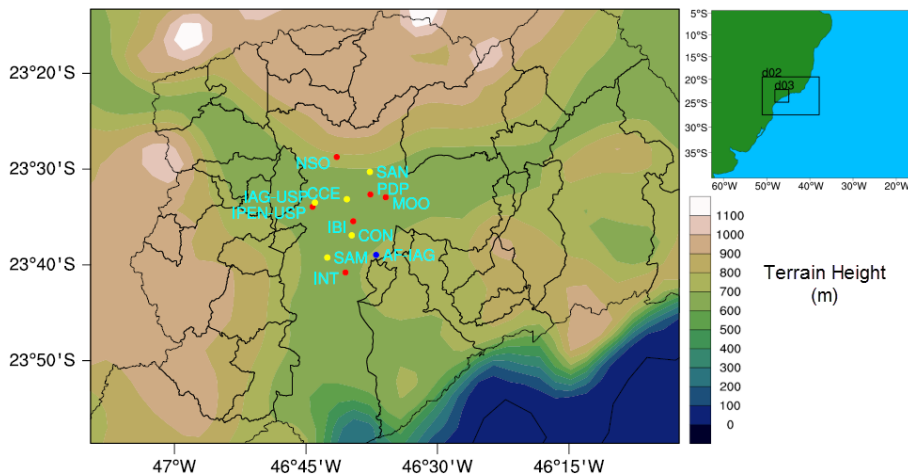


Figure 1. Downtown area of the 3 km modelling domain (d03) showing the locations of measurement sites in the vicinity of SPMA. Red dots represent sites with information of O₃ and aerosol. Yellow dots represent only sites with information of PM. Blue dot represents the location of the IAG-USP's climatological station.

A numerical study with the WRF-Chem model

A. Vara-Vela et al.

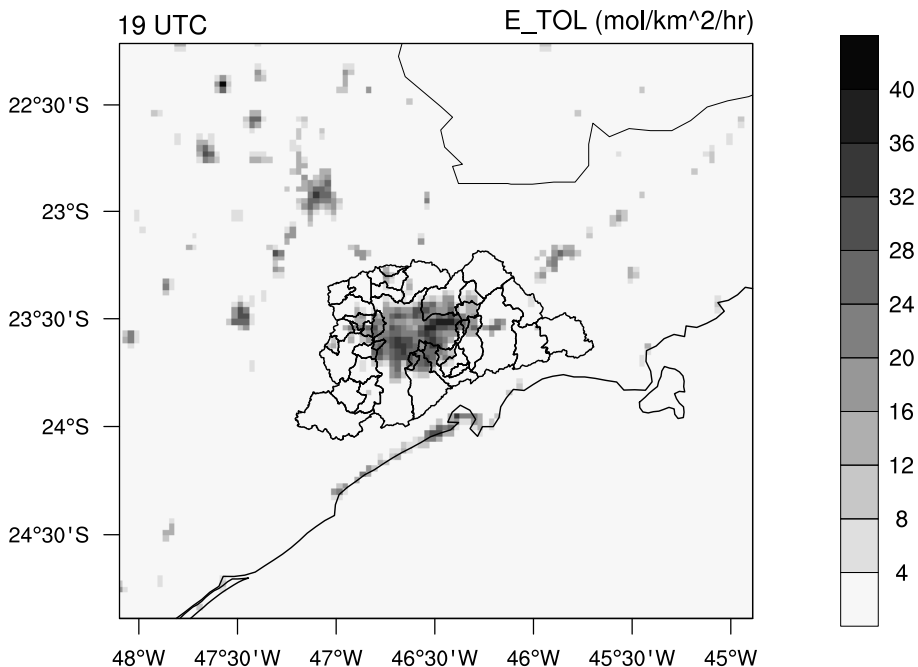


Figure 2. Emission rates for Aromatic VOCs at 19:00 UTC in the 3 km modelling domain.

14204

[Printer-friendly Version](#)

Interactive Discussion



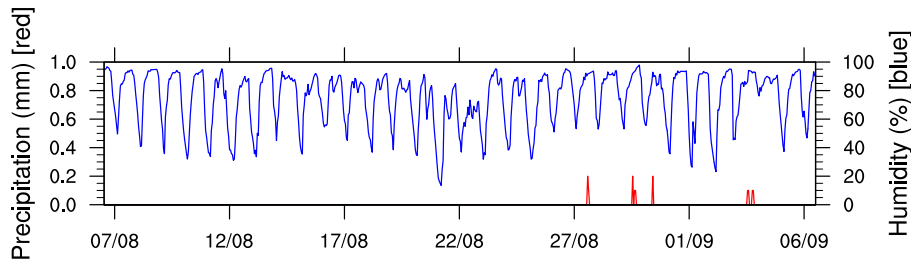


Figure 3. Accumulated daily precipitation and humidity observed at the IAG-USP's climatological station during the study period.

- [Title Page](#)
- [Abstract](#) [Introduction](#)
- [Conclusions](#) [References](#)
- [Tables](#) [Figures](#)
- [◀](#) [▶](#)
- [◀](#) [▶](#)
- [Back](#) [Close](#)
- [Full Screen / Esc](#)
- [Printer-friendly Version](#)
- [Interactive Discussion](#)



**A numerical study
with the WRF-Chem
model**

A. Vara-Vela et al.

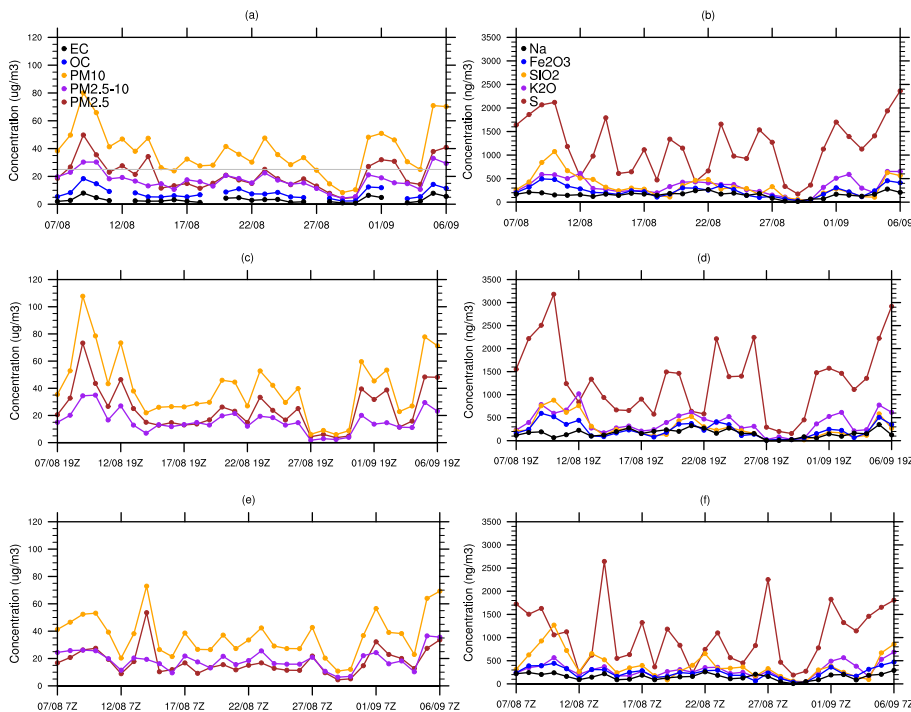


Figure 4. Daily mean concentration for some constituents of aerosol. The grey line indicates the WHO air quality standard for $\text{PM}_{2.5}$ ($25 \mu\text{g m}^{-3}$).

**A numerical study
with the WRF-Chem
model**

A. Vara-Vela et al.

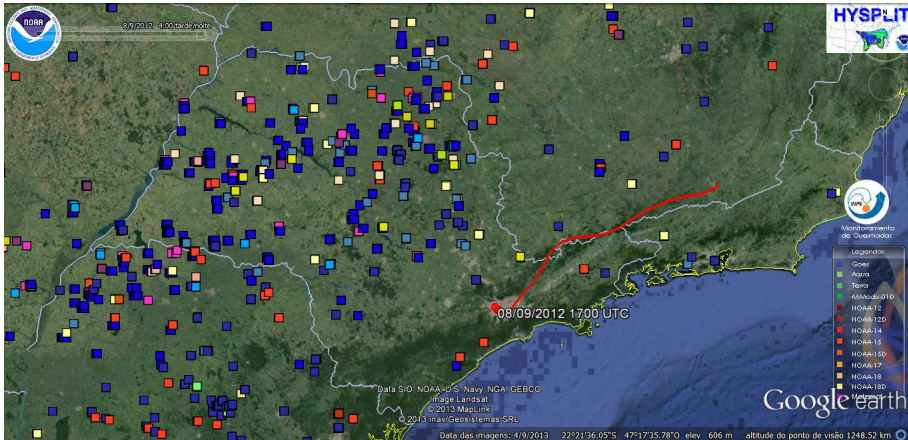


Figure 5. Air mass back trajectory and locations of fires on 9 August.

[Title Page](#)[Abstract](#)[Introduction](#)[Conclusions](#)[References](#)[Tables](#)[Figures](#)[Back](#)[Close](#)[Full Screen / Esc](#)[Printer-friendly Version](#)[Interactive Discussion](#)

Figure 6. Predicted average surface distribution of temperature and wind for the 3 km modelling domain. Blue dots and cyan numbers represent the locations and observed mean temperatures at measurement sites, respectively.

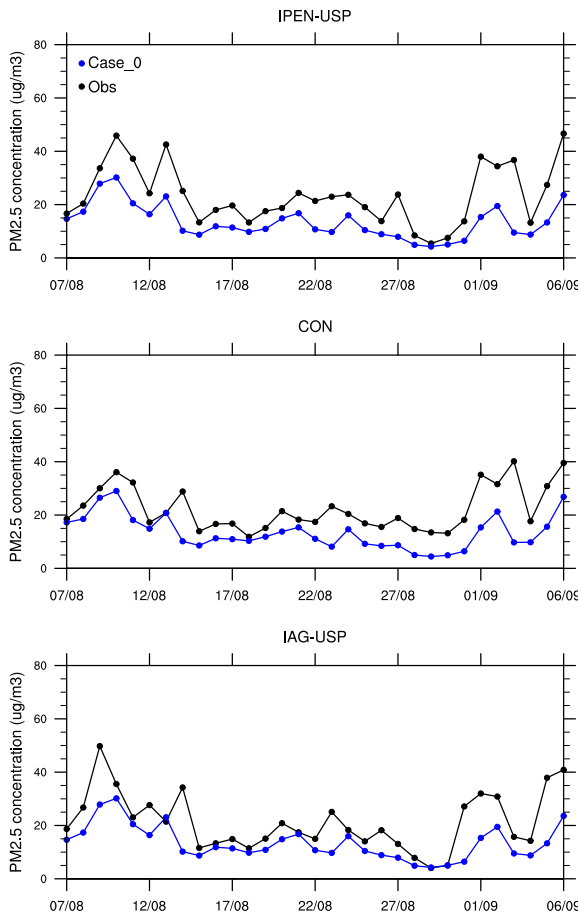


Figure 7. Observed and predicted daily variations of PM_{2.5} concentrations at 3 sites in SPMA for the 3 km modelling domain.

**A numerical study
with the WRF-Chem
model**

A. Vara-Vela et al.

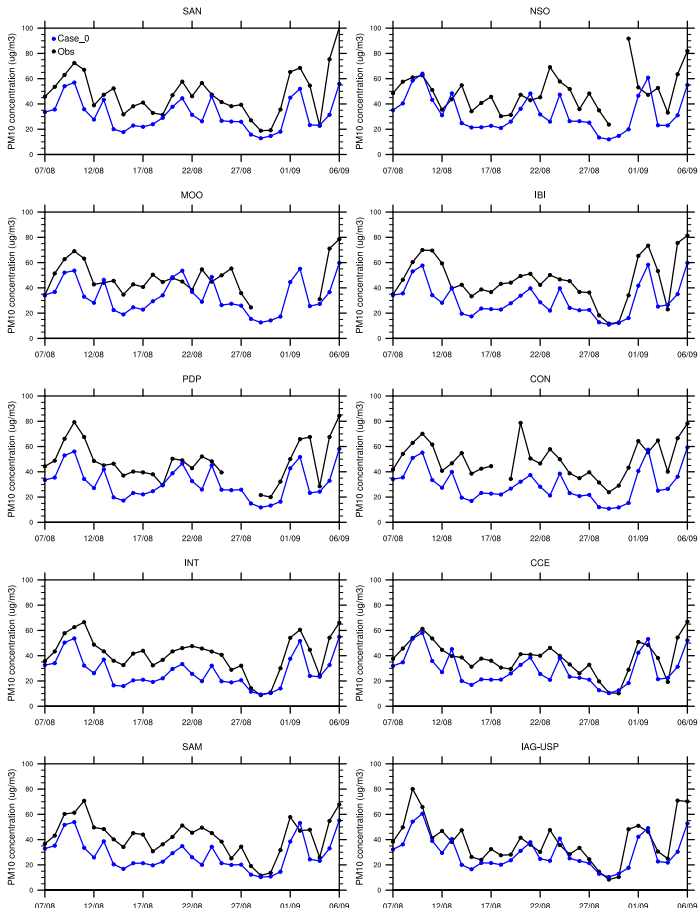


Figure 8. Observed and predicted daily variations of PM_{10} concentrations at 10 sites in SPMA for the 3 km modelling domain.



Title Page

Abstract

Introduction

Conclusions

References

Tables

Figures



Back

Close

Full Screen / Esc

Printer-friendly Version

Interactive Discussion

**A numerical study
with the WRF-Chem
model**

A. Vara-Vela et al.

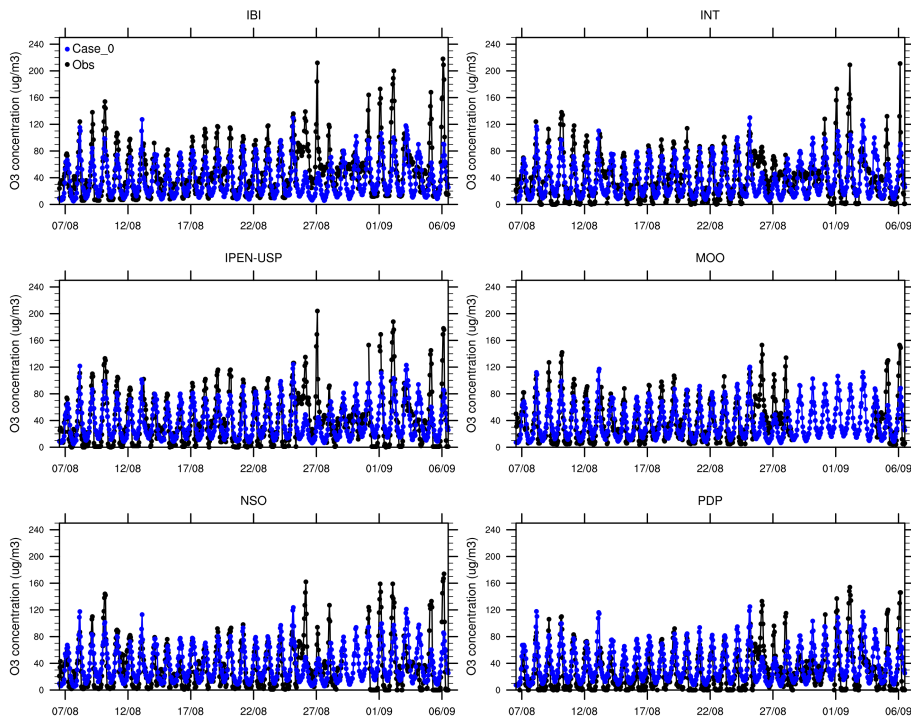


Figure 9. Observed and predicted daily variations of O₃ concentrations at 6 sites in SPMA for the 3 km modelling domain.

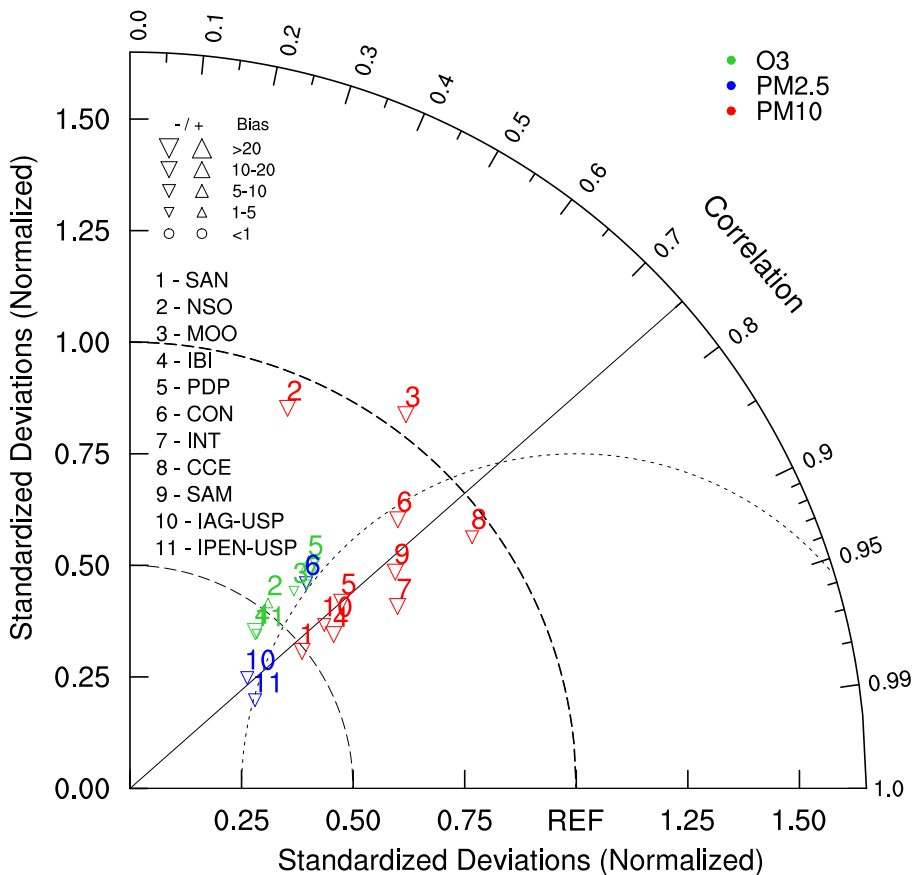


Figure 10. Taylor diagram for the PM_{2.5}, PM₁₀, and O₃ concentrations.

**A numerical study
with the WRF-Chem
model**

A. Vara-Vela et al.

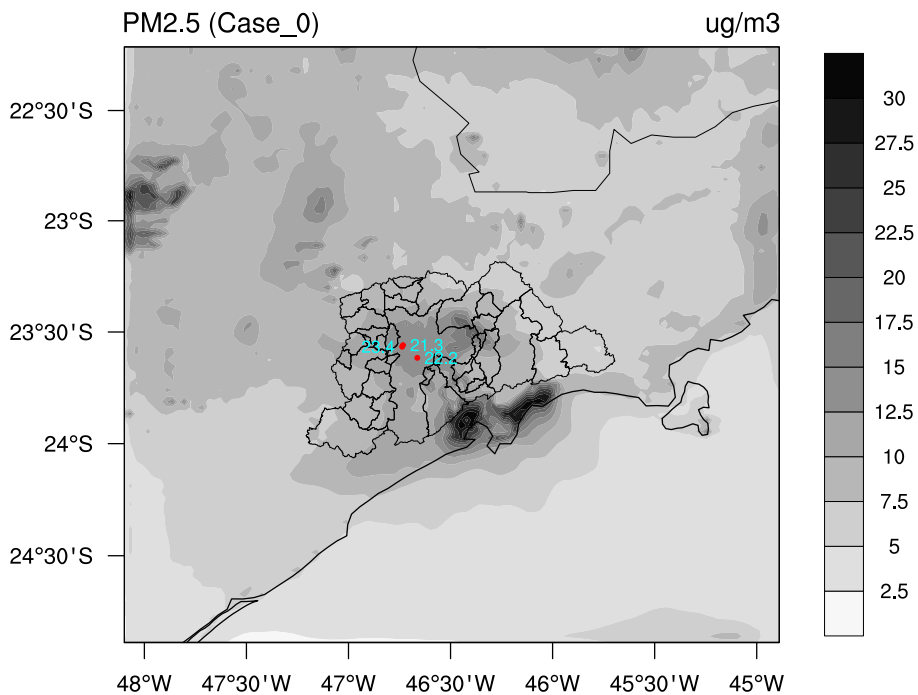


Figure 11. Predicted average surface distribution of PM_{2.5} concentrations for the 3 km modelling domain.

- [Title Page](#)
- [Abstract](#) [Introduction](#)
- [Conclusions](#) [References](#)
- [Tables](#) [Figures](#)
- [◀](#) [▶](#)
- [◀](#) [▶](#)
- [Back](#) [Close](#)
- [Full Screen / Esc](#)
- [Printer-friendly Version](#)
- [Interactive Discussion](#)



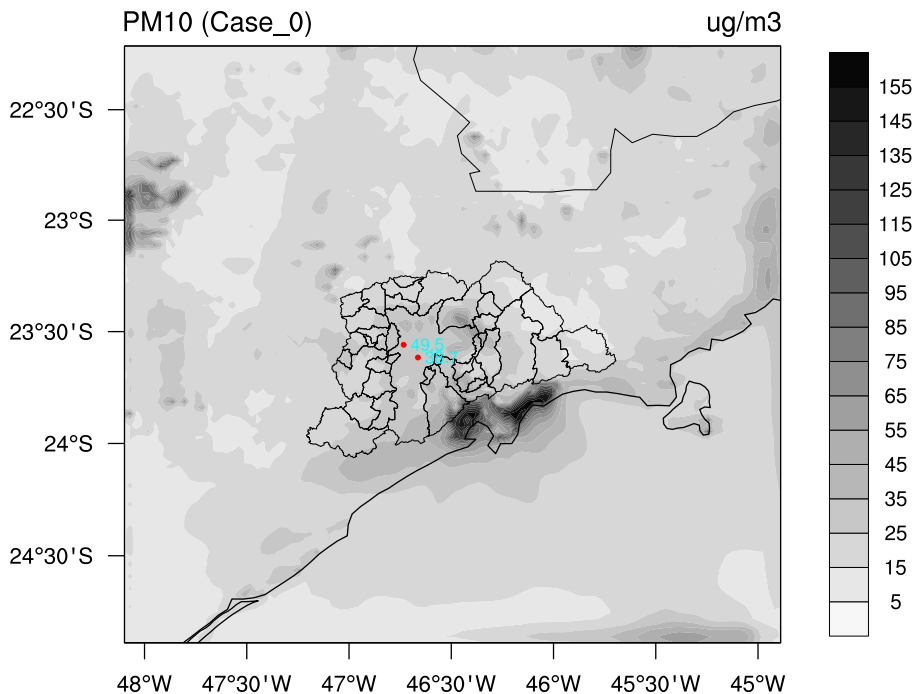


Figure 12. Predicted average surface distribution of PM₁₀ concentrations for the 3 km modelling domain.

**A numerical study
with the WRF-Chem
model**

A. Vara-Vela et al.

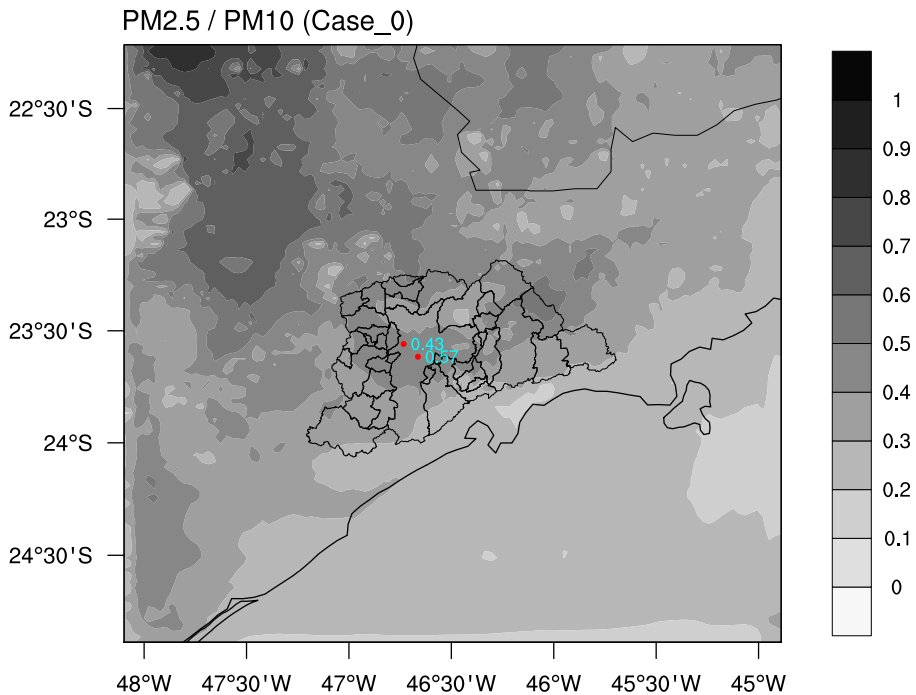


Figure 13. Predicted average surface distribution of the PM_{2.5} / PM₁₀ ratio for the 3 km modelling domain.

- [Title Page](#)
- [Abstract](#) [Introduction](#)
- [Conclusions](#) [References](#)
- [Tables](#) [Figures](#)
- [◀](#) [▶](#)
- [◀](#) [▶](#)
- [Back](#) [Close](#)
- [Full Screen / Esc](#)
- [Printer-friendly Version](#)
- [Interactive Discussion](#)

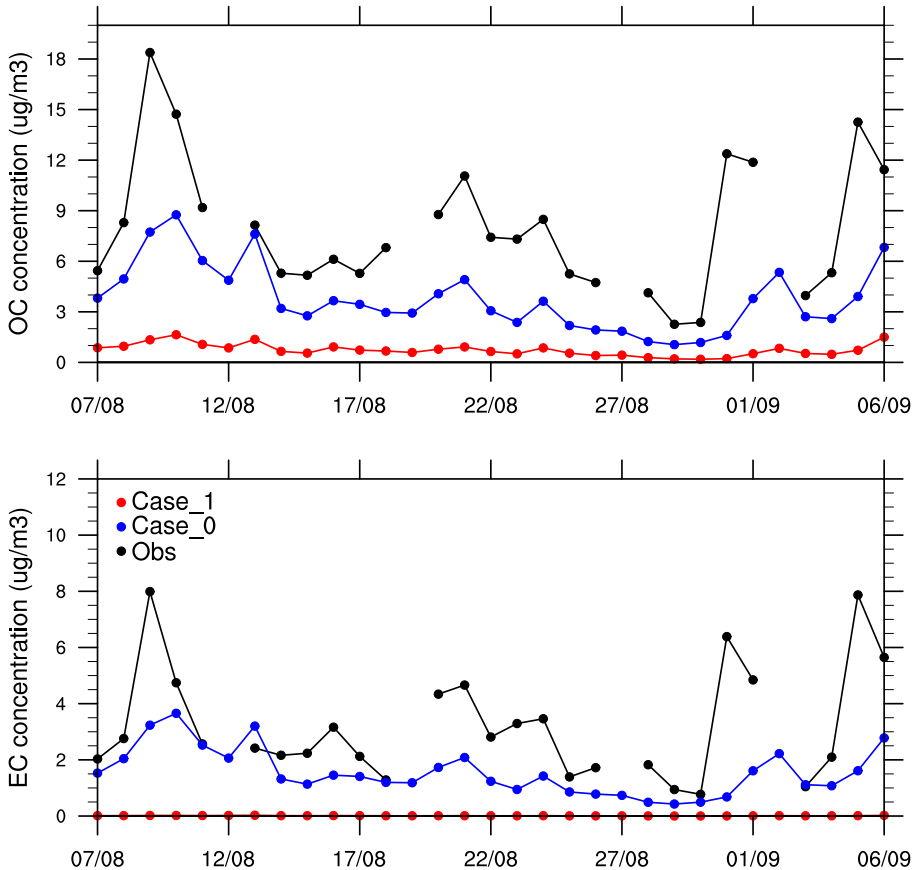


Figure 14. Observed and predicted daily variations of OC and EC concentrations at IAG-USP.

- Discussion Paper | Discussion Paper | Title Page | Abstract | Conclusions | Tables | Back | Full Screen / Esc | Printer-friendly Version | Interactive Discussion
- Discussion Paper | Discussion Paper | Introduction | References | Figures | Close



**A numerical study
with the WRF-Chem
model**

A. Vara-Vela et al.

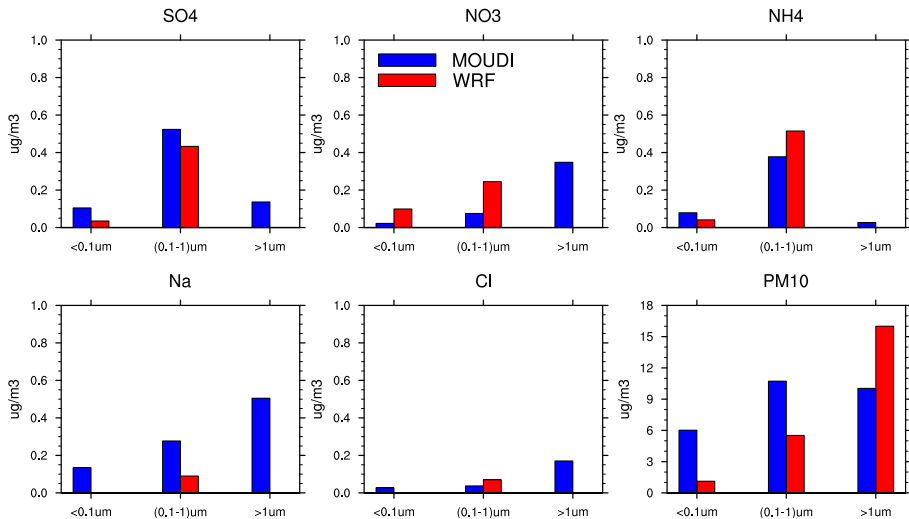


Figure 15. Observed and predicted average aerosol mass size distribution for SO_4 , NO_3 , NH_4 , Na , Cl , and other PM_{10} constituents at IAG-USP.

Figure 16. Observed and predicted average contributions for the main identified constituents of PM_{2.5} at IAG-USP.

**A numerical study
with the WRF-Chem
model**

A. Vara-Vela et al.

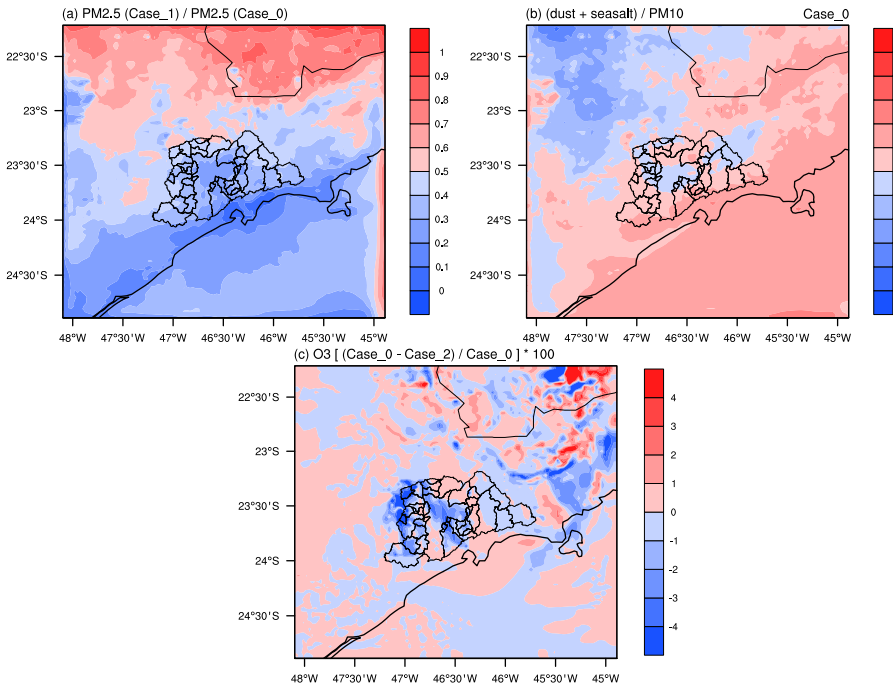


Figure 17. Contribution of (a) gas emissions on the fine particles formation, (b) dust-seasalt emissions on the PM₁₀ concentration, and (c) aerosol direct effect on the ground level O₃ concentrations at 16:00 LT.